

FRAGMENTS FROM THE CERN SPS Pb IONS AS A TEST BEAM FOR THE AMS RICH

M. Buénerd, L. Derome, R. Duperray, and K. Protasov
Institut des Sciences Nucléaires de Grenoble, IN2P3/CNRS

This document briefly outlines the main features of the secondary beam of ion fragments considered for the testing of the second generation RICH prototype of the AMS experiment.

Ideally, the ion test beam should cover the range of sensitivity of the RICH counter, i.e., provide:

- Isotopes over the mass range $A < \sim 30$ with $4 < P/A < 13$ GeV/c momentum per nucleon, to investigate the range of measurement capability for nuclear mass identification.
- Elements with Z lower than the upper (asymptotic) realistic limit for charge separation $Z < \sim 26$ (Fe region) to investigate the Z measurement capability (Cherenkov photons counting) of the counter.

In addition high Z ions are also interesting to test the overall response of the photodetection system to high charge particles.

SPS Beam line

The beam line used is H8 with T6 the production target. The beam conditions expected are as follows ¹ :

- Primary Pb beam intensity on production target 10^7 s^{-1} .
- Production target : Be from 10 cm ($0.25 \text{ }_1(\text{proton})$), $4 \text{ }_1(\text{Pb})$) to 30 cm.
- Angular acceptance of the H8 transport line: $\theta_{\text{max}} \sim \text{msr}$
- Maximum momentum acceptance of the H8 transport line: $P/P \sim 1.5\%$

It must be noted that the momentum resolution of the beam line can be set within the range $0.15\% < P/P < 1.5\%$, i.e., including the value expected for the AMS02 tracker ($\sim 1\%$) over the momentum range of isotopic mass resolution of the RICH. It is then particularly well suited for the test of the latter.

Beam fragments rates on target

The fragment rates can be evaluated on the basis of existing data and models of proven validity. Basically, the light fragments produced in Pb+A collisions will originate from two dominant mechanisms : Nuclear coalescence for low and intermediate momentum fragments, and nuclear limiting fragmentation at high momentum (\sim beam velocity). The spectrum of secondary protons however, would extend over the whole range available between target and projectile rapidities, being maximum at the two ends of the spectrum. To the opposite, no significant $A > 2$ fragment yield is expected within the intermediate rapidity range (see fig.4).

1. Beam rate for low momentum light (coalescence) fragments

Several recent experiments for various ion systems at high energies have shown that the coalescence yield for a given nuclear mass A , is decreasing as $Y^{-(A-1)}$, with Y increasing with the increasing beam energy. This means that the production rate of a fragment of mass $A+1$ is Y times smaller than the production rate of the fragment A . The empirical value of Y has been found to be $Y \sim 48$ at 11.5 GeV/n^2 , and ~ 200 for 158 GeV/n^3 , in accordance with the general trend observed for the coalescence coefficients to decrease at ultra relativistic energies for heavy systems ⁴. These numbers show that the 20 GeV/n beam is much more favourable for the production of light nuclear masses ($A \sim 2-4$) than the 158 GeV/n beam.

The rate estimate for the 158 A GeV beam has been made on the basis of the light mass $A \sim 1-3$ production yield measured in the NA44 experiment at CERN ³ (see appendix). Using the production cross sections

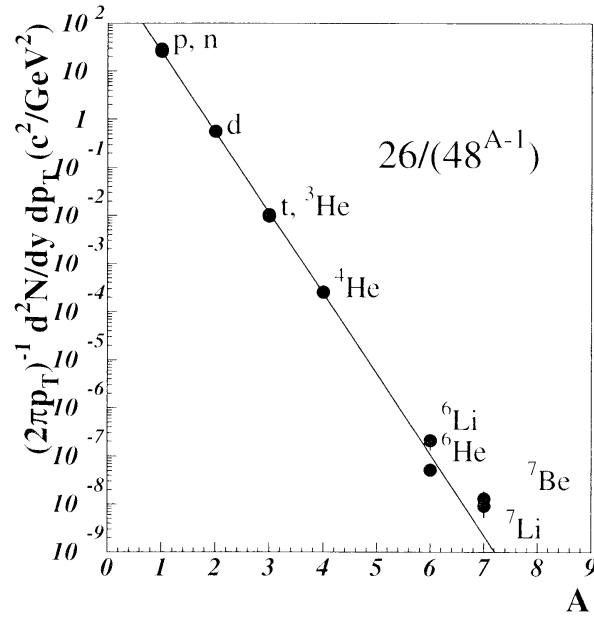


Figure 1 - *Light nuclei production at intermediate rapidity $y \sim 1.9$ (coalescence yield) measured at small transverse momentum in Au+Pb collisions at 11.5 GeV/nucleon (ref 1).*

reported in this experiment, the values quoted above for the target thickness (10 cm), primary Pb beam intensity, beam line maximum momentum spread and solid angle acceptance, and the total reaction cross sections of the considered systems, the following approximate rates should be available on the detector for 8 GeV/nucleon particles: 250 protons per spill, 1 deuterium per spill, 1 ^3H - ^3He per hour, and 1 ^4He per week. These numbers show clearly that acceptable samples of light nuclear masses could be obtained only for $A < 3$ over a week of running time. These rates however should increase with the decreasing momentum of particles.

2. Beam rates for high momentum fragments

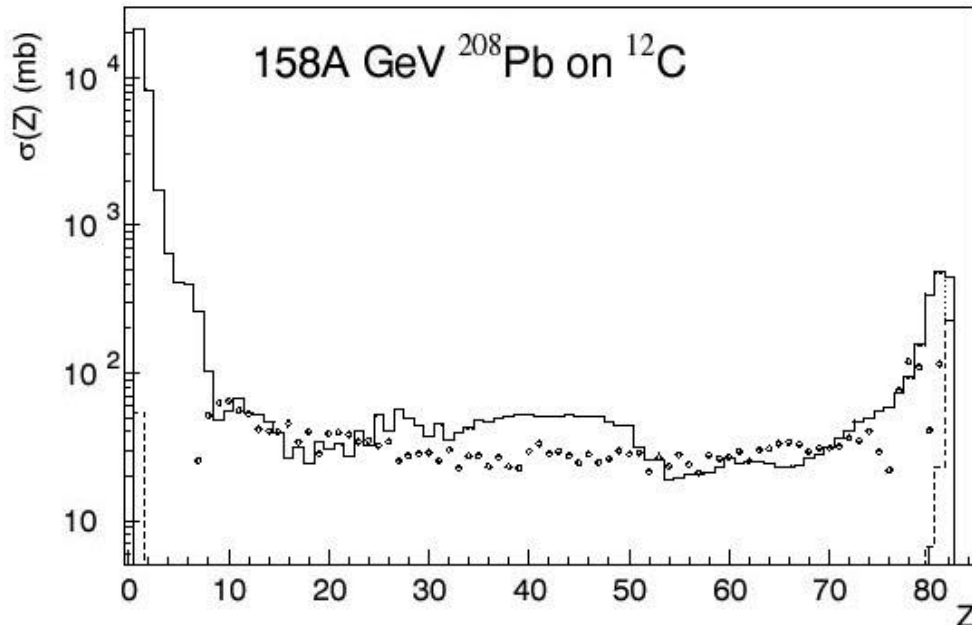


Figure 2 – *Projectile fragmentation cross sections as a function of the nuclear charge produced measured recently for $^{208}\text{Pb} + ^{12}\text{C}$ at 158 A GeV at the CERN SPS⁵ (symbols) and theoretical results from ref 6. Similar results are expected for 20 A GeV projectiles (see text)*

For estimating these rates, the recent data from ref ⁵ shown on figure 2 have been used and combined with the theoretical calculations of ⁶ (histogram on the figure).

The main dynamical features of the projectile fragmentation process can be inferred from the old Goldhaber model ⁷ which has widely proven to be successful at least for its gross features.

This is illustrated on Figure 3 where the fragment rapidity distributions for light fragments produced in Au collisions on a carbon target at 1 GeV/n ⁸ is shown to match the qualitative features of the fragmentation model. Although this incident energy is much below those to be used at CERN, the same features are expected in the present case since projectile fragmentation is a limiting process which becomes energy independent above less than 100 MeV/n incident energy.

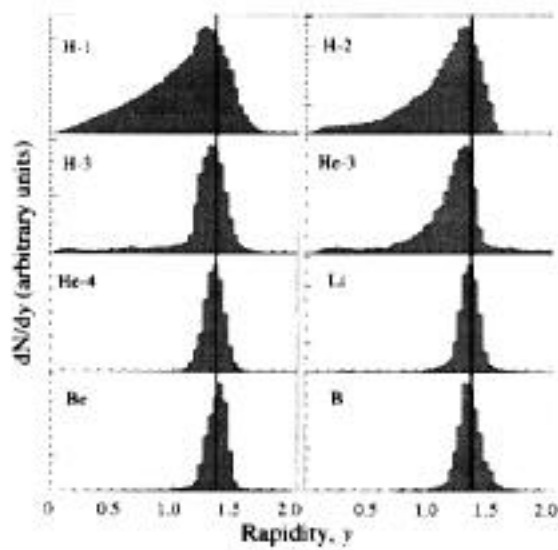


Figure 3 – Spectra of light nuclei produced by projectile fragmentation, measured in Au+C collisions at 1 GeV/n ⁸. Note that the rapidity distributions of the fragments are all centered on the beam rapidity with very little spread around this value, especially for the heavier fragments shown on the figure.

With the same beam line parameters already used for P/P and ^{208}Pb , and using the fragmentation cross sections given above, together with some simple qualitative estimates of the accepted angular and momentum distribution (see appendix), it can be evaluated that the count rate per nuclear element should easily be in the range of 10^3 particles per spill. This is more than needed for testing the velocity and charge resolution of the counter in various configurations with good counting statistics. Over the range of mass and charge of interest, it is seen from figure 2 above that the cross sections for He/C/Fe are in the approximate ratios 30/10/1, which is by the way not far from the cosmic ray relative intensities for these elements and thus remarkably suited to the present purpose. The corresponding ratios for rates depend somewhat on the target thickness as shown in the appendix, however.

3. Summary

Qualitatively, the beam situation is summarized schematically on figure 4 where the mass and energy distributions of the secondary nuclear fragments corresponding to the two production mechanisms discussed above, produced by primary Pb beam ions on the production target, are compared to the region of mass and charge separation to be investigated for the RICH prototype.

The beam fragmentation products all have the same velocity as the incident beam, extending over the whole range of mass from protons up to Pb. Nuclear masses produced above the region of interest for the RICH,

i.e., for $Z > \sim 25$, should be discarded from the beam line acceptance because of their larger charge to mass ratio as explained below.

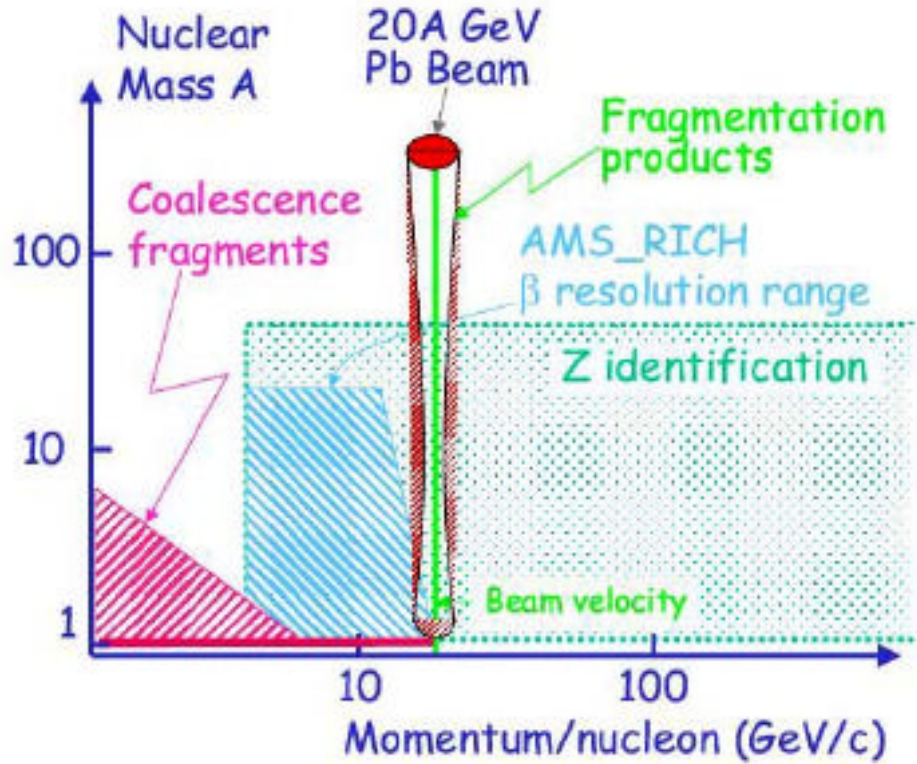


Figure 4 – Schematic representation of the secondary particle populations expected, compared to the domains of nuclear mass and charge to be investigated for the RICH prototype (see text for details).

It appears clearly on the figure that most of the expected range of mass identification of the RICH will not be covered by the available populations of secondary ions. However, the light nuclei ($A \sim 1-3$) flux produced by coalescence should allow to investigate the mass separation capability of the counter in the low momentum range of the RICH. Similarly, the light nuclei population ($A \sim 1-4$) produced by beam fragmentation will allow to explore the mass separation at the upper limit of the momentum range. This is an important test in view of the mass identification of light antimatter nuclei. In addition, the proton yield extending over the whole momentum range between coalescence and fragmentation could be used to investigate the response of the prototype through its whole momentum range from threshold up to the upper limit for mass identification of light nuclei $A < 4$, around 20 GeV.

For the 158A GeV beam, the beam position and fragmentation yield shown by the vertical mass distribution at 20 GeV on fig 4 would simply translate to the value 158 along the abscissa.

RICH prototype setup

The experimental setup will be very close to that shown on the figure below, which was used for the testing of the previous study prototype at the GSI Darmstadt facility⁹. The diameter of the vacuum chamber is 1 m, while the length along the beam line is of the order of 2 m. The apparatus will also include a set of scintillators and two small size MWPCs upstream of the chamber for trigger and tracking of particles respectively. In addition, one bay of electronics racks and another for gas distribution need to be installed close to the set-up as seen on the figure.

For the present setup, appropriate changes will be brought to the trigger and dE/dX detectors according to the following requirements :

- The amplitude dynamics for the dE/dX measurements by the scintillator counters should extend from $Z = 1$ up to $Z = \sim 25$. This corresponds to a value of about 100 taking into account that the energy loss dE/dX dynamics is of the order of 600, and that the light yield of the scintillator is quenched for highly ionizing particles reducing the dynamics by a factor of about 5-6 over this range of Z .

Thin radiator Cherenkov counters can also be used to this purpose. In this case a larger amplitude dynamics is required since the light yield is not quenched as for scintillators.

These dynamical ranges can be reached by combining responses from the anode and from the last dynode of the PMTs.

- A measurement of the beam particles time of flight (TOF) with a 70 m flight path will be performed to help on the mass reconstruction of the lightest incident particles ($A=1-2$).

A data acquisition system (DAQ) combining prototype front-end and processing electronics with the dedicated DAQ system of the future experiment controlled by a PC and a SUN computers, will be used. The terminals and an additional bay of electronics (NIM, VME, CAMAC crates) will be accommodated in the counting room.

The use of (Argon+CO₂) gas mixture is considered for MWPC operation. The experimental set-up is largely autonomous. Gas mixture, power, experimental area, and crane for installation will be required from CERN however.



Figure 5 - View of the experimental set up of the (1st generation) study prototype during the beam tests at GSI in April 1999. The same set up will be used at CERN for the second generation prototype.

Experimental procedure

The beam line will be tuned to transport particles with various rigidities from momenta per nucleon close to the RICH threshold (for aerogel 1.03 radiator, namely $> \sim 4\text{GeV}/c/n$) up to the momentum per nucleon of

Z_{beam} , and a velocity close to the beam velocity, $P/A = P_{\text{beam}}/A_{\text{beam}}$ (Lorentz factor). The beam rigidity is :

$$(B\rho)_{\text{beam}} = 3.33 P_{\text{beam}}/Z_{\text{beam}} = 3.1 A_{\text{beam}} (A/Z)_{\text{beam}} \quad (1)$$

obtained using $P \sim m_N \gamma v$, m_N being the atomic mass unit ($1 \text{ u} = 0.931 \text{ GeV}$), with B in T.m and P in GeV/c.

For the region of light nuclear masses we are interested in, the mass to charge ratio is $A/Z \approx 2$. The beam line will thus be set at the corresponding rigidity $(B\rho) = 3.1 A_{\text{beam}} (A/Z)$. In this case, the mass distribution of the fragmentation products transported to the detector will contain ^2H , ^4He , ^6Li , ^{10}B , ^{12}C , ^{14}N , ^{16}O , ..., ^{28}Si , ..., ^{40}Ca , etc.... Particular ions with $(A/Z) = (A/Z)_{\text{beam}}$, like ^7Be , ^{11}B , ^{13}C , ^{15}N , for example, can be obtained with a maximum yield by appropriate field settings of the line, satisfying the relation above. These data will be used to investigate the response in mass and charge of the counter.

One important question concerns the fragments produced with masses above the values of interest, i.e., between the Fe region and the mass of the projectile. In this range the yield is very large, especially around the projectile mass (see figure 2), and would overwhelm the counters if transported to the experiment by the beam line. Fortunately, it should not be the case thanks to the natural nuclear asymmetry: Stable nuclei above masses 40-50 have increasingly large nuclear asymmetry, i.e. $A/Z > 2$ ($A/Z \sim 2.5$ for Pb). The fragments produced over this range of mass with the projectile velocity will then have a rigidity larger than for $A/Z=2$ particles on which the beam line will be set. They will then not be transported to the detector.

Measurement program

The purpose of the run is to perform an end-to-end test of the prototype and to measure the response of the counter to ions over its mass, charge, and momentum ranges for particle identification, i.e., $1 < A < 25$, $1 < Z < 25$, $4 < P/A < 13 \text{ GeV/c}$. In particular, the following measurements are considered:

- **Velocity resolution** and corresponding mass resolution calculated with the measured value of the momentum measured by the beam line analysis (plus time of flight measurement independently for the lightest nuclei).
The study will be performed by means of :
 - a) Fragmentation products at the upper end of the momentum range of identification of light nuclei, namely $\sim 20 \text{ GeV/n}$, for the 20 A GeV Pb beam. The measurement will also be performed with ~ 1 fragments with the high energy 158 GeV/n beam.
 - b) Coalescence products (^1H , ^2H , ^3H , ^3He) in the low momentum range ($4 < P < \sim 8 \text{ GeV/n}$) both with 20 GeV/n (most favorable case) and 158 GeV/n beam.
- **Charge resolution**
- **Response to ions** in the upper (asymptotic) range of charge sensitivity (Fe) : This includes the study of the Rayleigh background generated, and the calibration of the counter for charge measurements.
- **Response to $Z=1$** particles over the momentum range $4\text{--}20 \text{ GeV/C/n}$, and counter reconstruction efficiency over this range.

In addition, the incident angle on the radiator could be varied and samples of data could be collected at angles within a 0 to 30° range of incidence (detector angle adjustable inside the chamber). This is important for investigating the charge reconstruction. Two or three Cherenkov radiators could be tested: silica aerogels with refractive index 1.03 and 1.05 , and NaF (sodium fluoride).

The details of the run plan will be elaborated in the forthcoming weeks.

APPENDIX

Calculations of secondary fragment rates available on the counter

In all the cases considered, all incident beam particles interact in the production target which length is $L \gg \lambda(\text{Pb})$.

- **Coalescence fragments:**

For the coalescence fragments, the rate n of particles available at the end of the beam line can be written as:

$$n = N_i \left(\frac{d^2 N}{dp d\Omega} \right)_{lab} p = N_i \frac{p^2}{E} \left(\frac{d^3 N}{dp^3} \right)_{inv}^{Pb+Be} p$$

where N_i is the beam intensity, incident $d^2 N / dp d\Omega$ the invariant multiplicity for the production of the considered nucleus in the beam-target collisions, and p and Ω , the momentum and angular acceptance of the beam line respectively.

Using the values of the invariant differential cross sections from ref [3] extrapolated to $p_t=0$ for protons ^1H ($10 \text{ GeV}^{-2}\text{c}^3$), deuterons ^2H ($6 \cdot 10^{-2} \text{ GeV}^{-2}\text{c}^3$), and tritons ^3H ($5 \cdot 10^{-4} \text{ GeV}^{-2}\text{c}^3$), and the total reaction cross sections for the Pb+Pb (8590 mb) and Pb+Be (3460 mb) systems, and making use of an empirical scaling with \sqrt{s} for the invariant multiplicities, one gets the following approximate rates for 8 GeV/c particles for the beam line parameters given above:

protons: 240 per spill; deuterons : 1 per spill; tritons and ^3He : 1 per hour. For ^4He the same calculation would provide about 1 particle per week.

In addition 8 GeV/c tritons are very rigid and would require a beam line setting below the nominal lower momentum limit.

- **Beam fragmentation :**

For the rates due to beam fragmentation, the relevant relation can be written (approximately) as:

$$n = N_i \frac{\sigma(F)}{\sigma_R} f\left(\frac{p}{p_0}\right) f(\theta)$$

where $\sigma(F)$ and σ_R are the production cross section of the fragment F and the total beam-target reaction cross sections respectively, while f and f' are the fractions of the momentum and angle distributions (assuming the factorisation assumption made here holds) accepted in the transport line respectively. As seen on figure 2 the fragment production cross section is of the order of 50 mb over the medium mass range of interest for the RICH, which roughly corresponds to $5 \cdot 10^4$ particles produced per spill at the target..

The two fractions can be estimated as follows:

- **Momentum and angular spread**

In the fragmentation model [7] the momentum distribution of the produced fragments with mass M in

the center of mass of the projectile, is gaussian with a rms value $\sigma(P_{lab}, A_p)$ depending on the fragment and projectile mass numbers A_f and A_p , and of the nuclear Fermi momentum:
 $\sigma^2 = \sigma_0^2 A_f(A_p - A_f)/(A_p - 1)$, with σ_0 being of the order of 90 MeV.

Boosting the momentum to the lab frame and taking into account the characteristic longitudinal momentum spread of one σ unit, one gets:

$$p_{||}^{lab}(M_f) = \gamma p_{||}^{proj}(M_f) + \beta \gamma E^{proj}(M_f) \pm \gamma \sigma + \gamma M_f$$

where the momentum spread appears thus to be of the order of $\sigma_0 A_f^{1/2}/M_f$ in the present case for light nuclear fragments, i.e., about 3%. This number is to be compared to the maximum momentum acceptance of the beam line of 1.5%. The fraction $f(\frac{p}{p})$ above is thus a sizable fraction of unity.

The angular slope can be estimated the same way: The characteristic transverse momentum is $\langle p_{\perp} \rangle \sim \sigma$. The one sigma unit angle of production of ^{12}C for example is thus $\sigma/P_{lab} \sim \sigma_0 A_f^{1/2}/P_{lab} \sim 1.2$ mrad for 20 GeV/n incident particles and one order of magnitude smaller at 158 GeV/n. Since the angular acceptance of the beam line is of the order of 1 mrad, the fraction $f(\quad)$ above is also not small compared to unity.

Taking ansatz values of 0.1 for both f and f' leads to beam rates of the order $5 \cdot 10^2$ per spill for a given transported element. These numbers show that required beam rates of the order of a few 10^2 per spill allowing statistically significant tests of the RICH prototype should easily be obtained in these experimental conditions.

The produced fragments interacting again in the target according to their particular interaction length, the flux emerging from the target has to be evaluated by a (simple) transport equation. The resulting flux for beam fragmentation is shown on figure 6 as a function of the target thickness, where it is seen that the relative rates between high and low Z fragments is decreasing with the increasing thickness of the target. For Fe/Li this ratio varies from about 10^{-2} for a 5 cm target down to about $2 \cdot 10^{-3}$ for 30 cm.

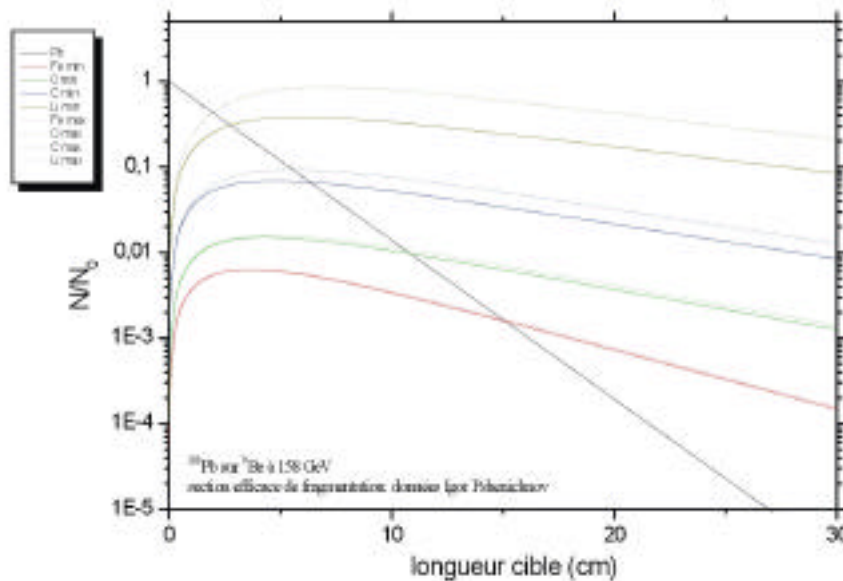


Figure 6 - Beam rates available at target exit as a function of target thickness, as obtained from simple transport calculations.

¹ Reference values from I.Efthymiopoulos, CERN MD.

² T.A. Armstrong et al., Phys. Rev. Lett. 83(1999)5431

³ A.G. Hansen et al., Nucl. Phys. A661(1999)687c; G. Ambrosini et al., NA52 preprint.

⁴ See for example I.G. Bearden et al., Nucl. Phys. A 661(1999)55c

⁵ S. Cecchini et al., hep-ex/0201039, Jan 2002.

⁶ I.Pshenichnov and K. Sümmerer, private communication; see also K. Sümmerer and B. Blank, nucl-ex/9911006; C. Scheidenberger, I.A. Pshenichnov, K. Sümmerer et al., submitted to Phys Rev C

⁷ A.S. Goldhaber, Phys. Lett. B 53(1974)306

⁸ J.A. Hauger et al., Phys. Rev. C57(1998)764

⁹ T. Thuillier et al., Nucl Inst and Meth in Phys A, in press ; astro-ph/0201051.